One pot stimuli-responsive linear waterborne polyurethanes via Diels-Alder reaction

June Aizpurua[a], Loli Martin[b], Elena Formoso[c,d], Alba González[a], Lourdes Irusta[a]

[a] POLYMAT, Polymer Science and Technology Department, Faculty of Chemistry, University of the Basque Country, UPV/EHU, 20018 Donostia, Euskadi, Spain.

[b] Macrobehaviour-Mesostructure-Nanotechnology SGIker Service, Polytechnic School, University of the Basque Country UPV-EHU, Plaza Europa 1, 20018. Donostia/San Sebastian, Spain.

[c] Farmazia Fakultatea, Kimika Fisikako Saila, Euskal Herriko Unibertsitatea (UPV/EHU), 01006 Vitoria-Gasteiz, Euskadi, Spain

[d] Donostia International Physics Center (DIPC), 2018 Donostia, Euskadi, Spain

Corresponding author's email address: lourdes.irusta@ehu.eus

ABSTRACT: Different strategies were used to obtain waterborne polyurethanes containing Diels-Alder moieties. In the first one (two pot), furan and maleimide end capped waterborne polyurethane dispersions were synthesized with the aim of obtaining a stimuli-responsive material after drying a mixture of both dispersions. However, the maleimide hydrolysis that took place at basic pH prevented the use of this strategy. The only way to introduce maleimide groups in the furan capped dispersions was after water removal, which limits the application. In the second strategy (one pot), a Diels-Alder adduct was introduced in the polyurethane chain. Using this strategy, stable waterborne polyurethane dispersions were successfully synthesized.

Both strategies allowed the obtaining of films that according to FTIR, DSC and NMR experiments showed cyclic temperature responsive behaviour, as at high and low temperature the Diels-Alder adduct was opened and regenerated respectively. As a consequence of this reaction, the temperature increase provoked chain scission reducing both the polymer molecular weight and the viscosity.

Using the one pot strategy, a Diels-Alder adduct containing polyurethane film was obtained for the first time from waterborne systems. This can be of great interest in order to obtain functional self-healing coatings with reduced volatile organic compounds (VOC).

Keywords: Waterborne Polyurethane, Diels-Alder, Stimuli-responsive, One Pot

Introduction

Organic coatings are designed to protect subtracts from the environment by creating a barrier layer. However, the current coatings (called functional coatings or smart coatings) are designed not only for surface protection but also for additional functions or properties such as self-healing and self-cleaning.

Currently, the coatings industry faces different challenges, among which the development of multifunctional and sustainable coatings is highlighted [1].

One of the most desirable properties for a coating is its self-healing ability [2–6]. Coatings having this property are able to repair scratches autonomically or by the application of a stimulus such as temperature or UV irradiation [7].

There are different ways of introducing the self-healing ability to the materials. Among them, the introduction of Diels Alder moieties is one of the most employed [8–10]. The reaction between furan (diene) and maleimide (dienophile) moieties is a thermally reversible reaction (Diels-Alder reaction) that gives rise to the formation of a cyclohexene ring (DA adduct). The temperature reversibility of this reaction enables the joining or separation of the furan /maleimide bonds in a controlled way, selecting the appropriate temperature conditions [11]. Thus, in linear polymers containing DA moieties, the temperature induced Diels-Alder and retro Diels-Alder reactions provoke the increase or decrease of the molecular weight. The temperature induced changes can be used to obtain self-healing polymers since the low molecular weight species formed as a consequence of the retro Diels-Alder reaction can diffuse easily and lead to fast healing that cannot occur in the high molecular weight linear polymers. In the case of cross-linked polymers containing DA moieties, the retro Diels-Alder reaction induces a reduction of the crosslinking density, which also increases the chain diffusion enabling not only sample healing but also the recycling of the cross-linked network. These materials, which referred to as covalent adaptable networks (CANs), are promising cross-linked materials that can be repeatedly healed or recycled using appropriate temperature cycles.

Taking advantage of the Diels-Alder reaction, different materials have been developed showing self-healing ability. Diels-Alder reaction has also been extensively used in polyurethane chemistry. Some authors report the formation of furan capped polyurethanes that are chain extended [12,13] or cross-linked [14–18] with bismaleimide compound to give rise to temperature responsive self-healing polyurethanes. There are also works where, using a similar strategy, a maleimide capped polyurethane is cross-linked by means of a furan compound [19–21] or maleimide and furan capped polyurethanes are mixed [22]. Other authors, instead of using the furan/maleimide mixture, introduce the DA moieties into the polyurethane backbone using modified diols [23–25]. This approach is especially interesting as it reduces the reaction steps allowing the one pot synthesis. Finally, it is worth mentioning that recently DA moieties have been introduced in non isocyanate based polyurethanes [26].

The self-healing abilities can be improved if the material presents shape memory effect. Thus, in a scratched sample, the shape memory effect can help to repair the scratch. Following this

idea, different shape memory polyurethanes containing DA moieties are described in literature [27–32].

It is clear from the above that DA moieties have been successfully introduced in polyurethanes to give rise to self-healing linear and cross-linked polymers. However, there is a lack of papers devoted to the synthesis of environmentally friendly self-healing polyurethane dispersions. Thus, there are some works where self-healing waterborne polyurethanes based on coumarin [33] and disulphide [34] healing chemistry are described, but currently the introduction of DA moieties in waterborne polyurethanes has not been described. Taking this into account, the present work is devoted to obtaining these types of functional and sustainable coatings. This development will allow environmentally friendly polyurethane functional smart coatings with self-healing abilities based on Diels-Alder chemistry to be obtained for the first time. Thus, two different strategies are presented based on the well-known "acetone process" [35–37]. In the first one, furan and maleimide end capped polyurethane dispersions were synthesized with the aim of obtaining a stimuli-responsive material after drying a mixture of both dispersions. In the second strategy (one pot), a Diels-Alder adduct was introduced into the polyurethane chain.

Experimental

Materials

Isophorone diisocyanate (IPDI), 2-bis (hydroxymethyl) propionic acid (DMPA), 1,4-butanediol (BD), polypropylene glycol (PPG) (Mn 1000 g/mol and 425 g/mol), triethylamine (TEA), dibutiltin diacetate (DBTDA), ethanolamine, furfuryl alcohol (FA), furfuryl amine (FAM), 1,1′-(methylenedi-4,1-phenylene) bismaleimida (BMI), acetone, methanol, ethanol and toluene were purchased from Sigma-Aldrich Chemical Corporation. Exo-3,6-Epoxy-1,2,3,6-tetrahydrophthalic anhydride was purchased from TCI Europe N.V.

Synthesis of N-(2-Hydroxyethyl) maleimide (MA)

In order to obtain a maleimide compound containing a hydroxyl group, two reactions were carried out as described in literature [38].

In the first reaction, 6 g (0.036 mol) of exo-3,6-epoxy-1,2,3,6-tetrahydrophthalic anhydride was suspended in 100 mL methanol in a round-bottom flask and the suspension was cooled to 0 °C. Next, a solution of 2.206 g (0.036 mol) of ethanolamine in 40 mL methanol was added drop by drop to this cooled mixture. After 10 min stirring, the solution was warmed to room temperature, left for an additional 1 h, and next refluxed for 3 h. Finally, the mixture was cooled to room temperature, and the solvent was removed under reduced pressure (80 mbar at 60 °C). The product was crystallized from ethanol.

In the second reaction, the obtained product was suspended in 100 mL toluene in a round-bottomed flask and was refluxed for minimum 10 h. Afterwards, the mixture was cooled down to room temperature and the solvent was removed under reduced pressure (80 mbar at 90 °C). The product was crystallized from toluene.

^{1}H NMR (300 MHz,$CDCl_3$)) δ (ppm) 6.74 (s, 2H), 3.78 (t, 2H), 3.73 (t, 2H), 1.66 (s,1H).

Synthesis of 2-(2-hydroxyethyl)-4-(hydroxymethyl)-3a,4,7,7a-tetrahydro-1H-4,7-epoxyisoindole-1,3(2H)-dione (DA2OH)

DA adduct containing two hydroxyl groups was synthesized as described in literature [24].

The reaction was carried out in 100 mL toluene in a flask reactor. 10 g (0.0710 mol) of N-(2-hidroxyethyl maleimide) and 7.1 g (0.0724 mol) furfuryl alcohol were mixed in the reactor and the reaction temperature was raised up to 80 °C. The reaction was carried out for 24 h under mechanical stirring, during which the product precipitated. The resulting mixture was cooled to room temperature. Then the product was collected via vacuum filtration and washed with diethyl ether.

^{1}H NMR (300 MHz, d_6-DMSO)) δ (ppm) 6.53 (br, 2H), 5.09 (s, 1H), 4.94 (t, 1H), 4.77 (t,1H), 4.07-3.67 (dd, 2H), 3.41 (br, 4H), 3.04 (d, 1H), 2.90(d, 1H).

Synthesis of temperature stimuli responsive waterborne polyurethanes (WPU)

Waterborne polyurethane dispersions were prepared in two main steps. In the first step, the polymer was synthesized, and in the second one, the dispersion process was carried out.

A series of polyurethanes were synthesized, furan capped (PUFAM), maleimide capped (PUMA) and DA adduct containing (PUDA) polyurethanes. All the reactions were carried out in a 250 mL jacket glass reactor equipped with a mechanical stirrer and a condenser. Acetone was used as solvent to carry out the synthesis for PUMA and PUDA.

Synthesis of furan capped (PUFAM) and maleimide (PUMA) capped polyurethanes

The synthetic way to obtain PUFAM and PUMA polymer is shown in Scheme 1. Polyol (PPG Mn=1000 g/mol for PUFAM (18 g, 18 mmol) and Mn=425 g/mol for PUDA (7.65 g, 18 mmol)), internal emulsifier (DMPA, 1.18 g, 8.8 mmol), and the required amount of TEA to completely neutralize DMPA acidic groups were fed into a 250-mL jacket glass reactor equipped with a mechanical stirrer together with DBTDA (800 ppm). For PUMA 30 wt % acetone was used as solvent. When the reaction temperature reached 57 ^{o}C for PUMA and 70 ^{o}C for PUFAM, IPDI (10 g, 45.2 mmol) was added. The mixture was stirred at these temperatures for 3 h and then the polymer chains were extended using the appropriate amount of BD, leaving some free isocyanate groups. This reaction was carried out for one additional hour. Next, FAM or MA was added to react with residual NCO groups. The reaction was periodically monitored by Fourier transform infrared spectroscopy (FTIR) and it was stopped when the infrared absorbance of the NCO groups (around 2260 cm^{-1}) was negligible. The reagent amounts used in the different reactions are summarized in Table 1 and Table 2.

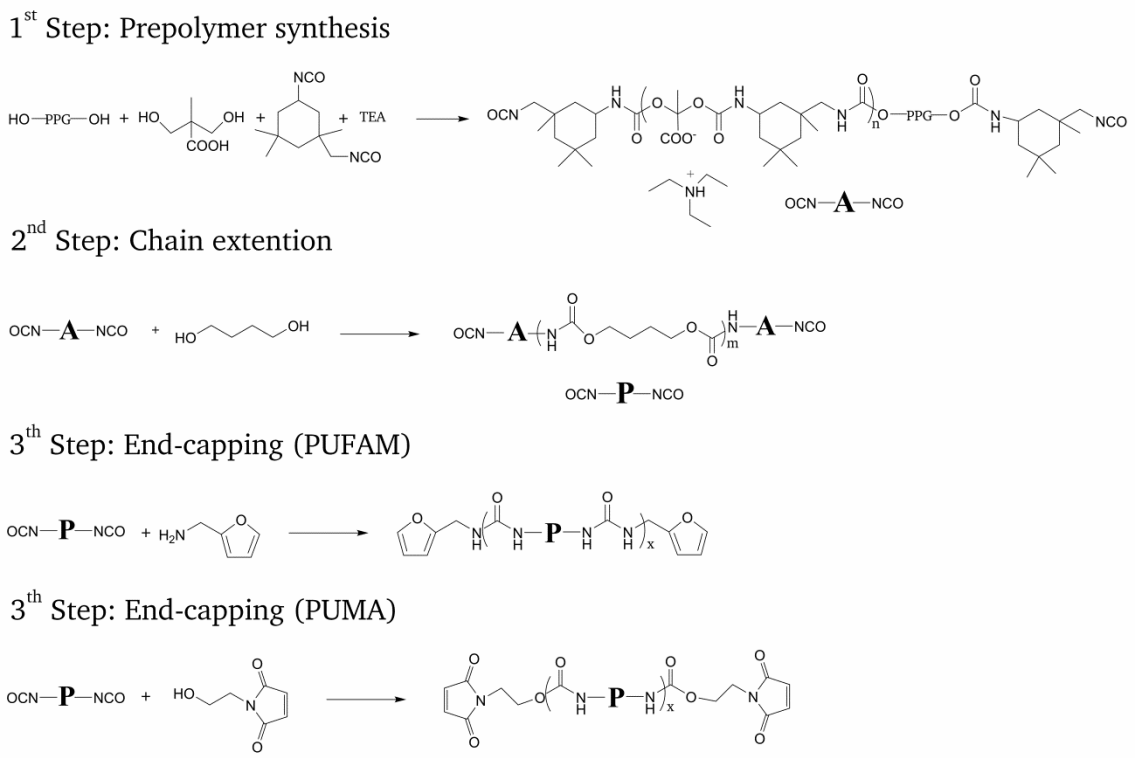

Scheme 1 Synthetic pathway to obtain PUFAM and PUMA polyurethanes.

Polymer	PPG (mmol)	DMPA (mmol)	IPDI (mmol)	TEA (mmol)	BD (mmol)	FAM compound (mmol)	(wt %)
PUFAM5	18.0	8.8	45.2	12.0	10.8	15.2	4.7
PUFAM7	18.0	8.8	45.2	12.0	6.4	24.0	7.3
PUFAM10	18.0	8.8	45.2	12.0	2.0	32.8	9.8

Table 1 Amount of reagents used in the synthesis of different PUFAM.

Polymer	PPG (mmol)	DMPA (mmol)	IPDI (mmol)	TEA (mmol)	BD (mmol)	MA compound (mmol)	(wt %)
PUMA6	18.0	8.8	45.2	12.0	10.8	15.2	10.5
PUMA10	18.0	8.8	45.2	12.0	6.4	24.0	16.1
PUMA14	18.0	8.8	45.2	12.0	2.0	32.8	19.5

Table 2 Amount of reagents used in the synthesis of different PUMA.

Synthesis of polyurethane bearing DA adduct (PUDA)

The synthetic way to obtain PUDA polymer is shown in Scheme 2. Polyol (PPG Mn=1000 g/mol, 18 g, 18 mmol), DA2OH (see table 3), internal emulsifier (DMPA, 1.18 g, 8.8 mmol) and the required amount of TEA (1.21 g, 12 mmol) to completely neutralize DMPA acidic groups, were poured together with DBTDA (800 ppm) and acetone (14 g) into the reactor. Once the reaction temperature reached 57 ^{o}C, IPDI (10.04 g, 45.2 mmol) was added. The reaction was maintained for 24 hours, and finally the required amount of chain extender (BD) was added to the reaction mixture in order to obtain stoichiometric ratio of NCO and OH groups. The reaction was periodically monitored by Fourier transform infrared spectroscopy (FTIR) and it was stopped when the infrared absorbance of the NCO group stretching vibration (around 2260 cm^{-1}) was negligible. The reagent amounts used in the different reactions are summarized in Table 3.

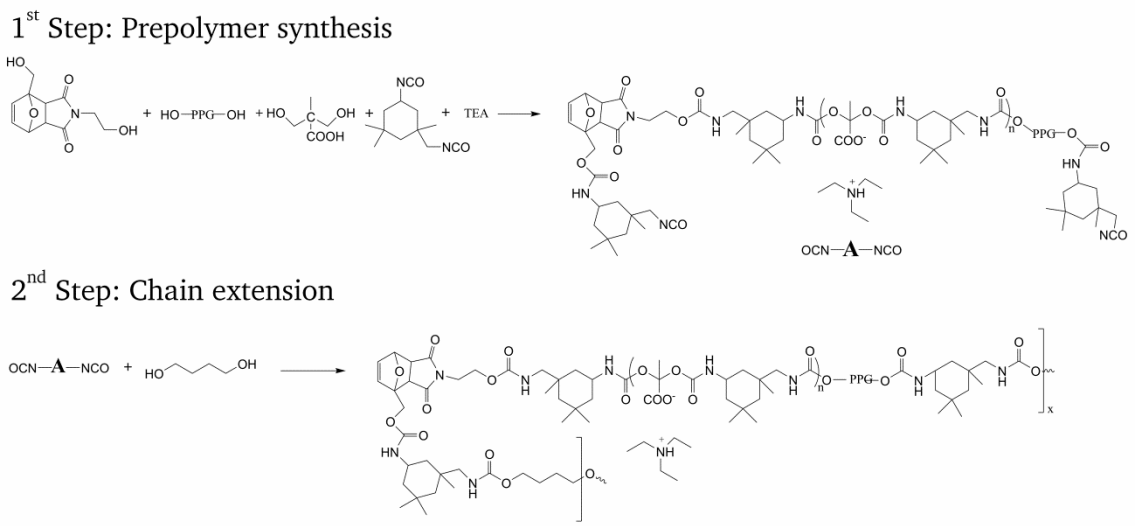

Scheme 2 Synthetic pathway to obtain PUDA polyurethanes.

Polymer	PPG (mmol)	DMPA (mmol)	IPDI (mmol)	TEA (mmol)	BD (mmol)	DA2OH compound (mmol)	DA2OH compound (wt %)
PUDA6	18.0	8.8	45.2	12.0	10.8	7.6	5.7
PUDA9	18.0	8.8	45.2	12.0	6.4	12.0	9.3
PUDA12	18.0	8.8	45.2	12.0	2.0	16.4	11.8

Table 3 Amount of reagents used in the synthesis of different PUDA.

Dispersion process

The emulsification process is highly dependent on experimental parameters, such as polymer concentration, emulsification temperature, water addition rate and solvent evaporation temperature [35,36,39]. In order to study the influence of the Diels-Alder moieties amount on the polyurethane water dispersion abilities, polymer dispersions in water were prepared under similar conditions. Therefore, before starting the dispersion process the polymer concentration was adjusted to 70 wt %, the temperature was maintained at room temperature (25 ^{o}C) and the mechanical stirring was raised to 300 rpm to help the dispersion process. In these conditions water was added drop-wise at 1.5 mL·min^{-1}. Once the dispersion was achieved, the solvent was removed using a rotary evaporator at 30 ^{o}C under vacuum. The solid content of the resulting dispersion was 20 wt %.

Instrumentation

Fourier Transform Infrared (FTIR) was used to follow the polyurethane polymerization process and to study the Diels-Alder reaction at different temperatures. FTIR spectra were recorded at different polymerization times at room temperature using a Nicolet 6700 spectrometer (Thermo Scientific) and a Nicolet MAGNA-IR 560 spectrometer equipped with a heater accessory (SPECAC), which was employed to perform the experiments at different temperatures. The spectra of films obtained by casting the solutions onto KBr pellets were registered at a resolution of 4 cm^{-1} and a total of 10 interferograms were signal averaged.

^{1}H liquid Nuclear Magnetic Resonance (NMR) spectra were obtained in a Fourier Transform Bruker 300 MHz spectrometer (model Avance 300 DPX) with deuterated chloroform ($CDCl_3$) as solvent. This technique was employed to confirm the structure of the polymers.

Dynamic Light Scattering (DLS) measurements were carried out using 90Plus (Brookhaven) Particle Size Analyzer in order to obtain the diameter of the particles.

Differential Scanning Calorimetry (DSC) study was performed in a TA Instruments Q 2000 from -80 to 180 ºC at a heating rate of 10ºC/min under nitrogen flow. A sample of about 7 mg was used for the measurements.

Size Exclusion Chromatography (SEC) analyses were performed in an Ultimate 3000 (Thermo Scientific) SEC equipped with a refraction index detector, RefractoMax 520 RI. The selected columns were Phenomenex Phenogels with a detection range from 100 to 10^6 g·mol^{-1}. Sample concentration on THF was 20 mg·mL^{-1}.

The rheological measurements were carried out in an Anton Paar Physica MCR101 rheometer. The device presents stress controller characteristics and the experiments were performed using 25 mm parallel plate geometry.

Computational details

The optimization of geometrical structures for the topological analysis were performed using Gaussian09 program [40]. The M06-2X [41] electron density functional and the cc-pVTZ basis set [42,43] were used as this combination has demonstrated to reproduce accurately Diels-Alder reactions [44]. To confirm that the optimized structures were real minima on the potential energy surfaces, frequency calculations were carried out at the same level of theory. All structures showed positive force constants for all the normal modes of vibration.

The interaction energy of the model polymers were defined as the energy balance of the reactions to obtain PUDA and PUFAM-BMI adduct, where the reactants were always calculated at the same theory level as the products.

The Non-Covalent Index (NCI) analysis [45] was carried out using to the NCIPLOT code [46]. The technique rest on the analysis and the graphical interpretation of the electronic density (ρ) and its derivatives, namely the λ_2 eigenvalue of its Hessian and its reduced gradient s(ρ), defined as:

$$s = \frac{1}{2 \cdot (3\pi^2)^{1/3}} \frac{|\nabla \rho|}{\rho^{4/3}}$$

Results and discussions

Characterization of PUFAM and PUMA

The evolution of the polymerization reaction was followed by FTIR. Figure 1 and Figure 2 show the infrared spectra corresponding to different steps of the reaction. As can be seen, the initial spectrum, which corresponds to the time when IPDI was added to the reaction mixture, is characterized by the strong band at 2260 cm^{-1} caused by the stretching vibration of isocyanate

groups. As the reaction progresses, this band decreases and the bands due to Amide I and Amide II of the urethane groups at 1710 cm^{-1} and 1550 cm^{-1} appear, together with the N-H stretching vibration (3330 cm^{-1}). In addition, in PUFAM synthesis when FAM was added a shoulder in the carbonyl band is observed (1650 cm^{-1}) due to urea formation (Figure 1). In PUMA synthesis when MA was added two bands at 830 cm^{-1} and 700 cm^{-1}, attributable to the o.o.p bending vibrations of the maleimide double bond, appear (Figure 2). The FTIR spectra of the final products do not present either the isocyanate or the OH vibration bands, which means that the polymerization reactions were performed successfully.

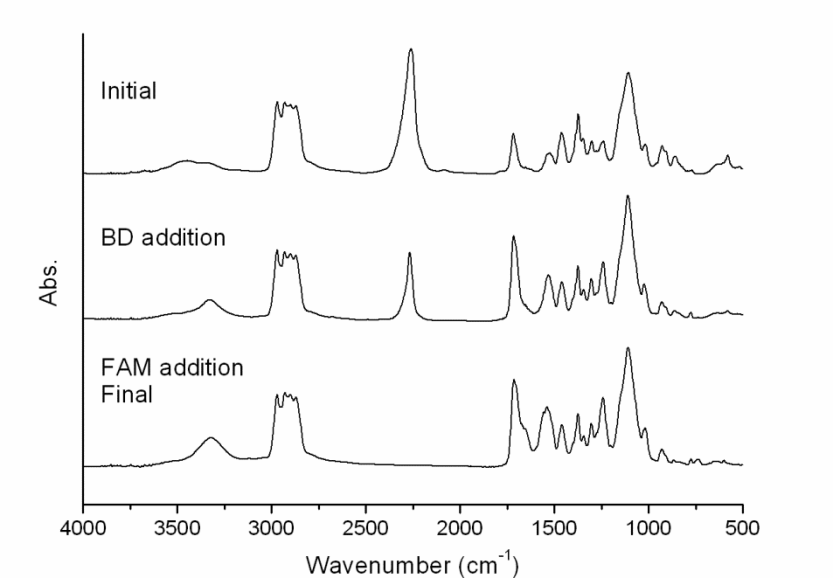

Figure 1 FTIR spectra at different reaction steps of PUFAM10 sample.

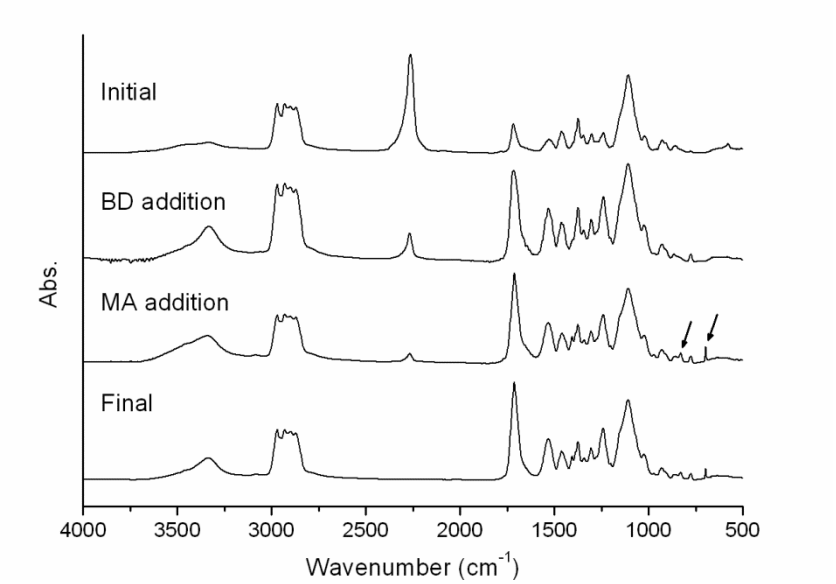

Figure 2 FTIR spectra at different reaction steps of PUMA10 sample.

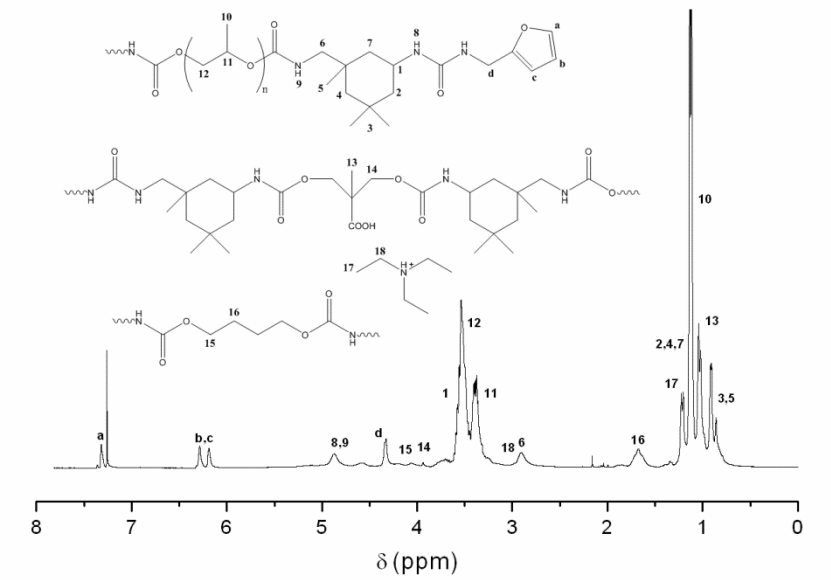

Figure 3 ^{1}H-NMR spectrum and line assignment for PUFAM10 sample.

The structure of the obtained polymers was confirmed by ^{1}H-NMR spectroscopy. The ^{1}H-NMR spectrum and the line assignment are shown in Figure 3 for PUFAM and in Figure 4 for PUMA. The region between 4.5 ppm and 3.5 ppm is particularly significant as it is the region where CH_2 protons directly attached to urea and urethane bonds appear. Thus, the presence of d (PUFAM samples) and c (PUMA samples) confirms the incorporation of the furan and maleimide monomers in the polymer structure.

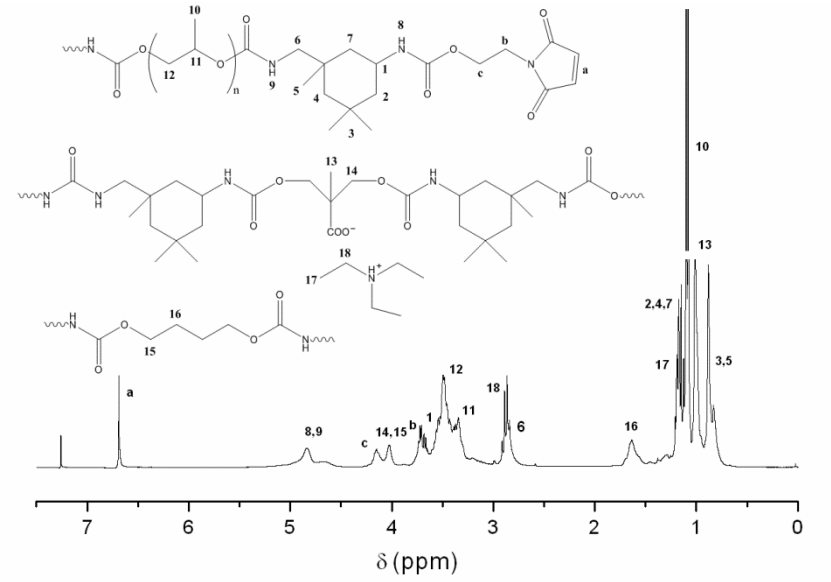

Figure 4 ^{1}H-NMR spectrum and line assignment for PUMA10.

Characterization of PUDA

Regarding the PUDA system, the polymerization reaction was also followed by FTIR and the characterization of the samples was made by ^{1}H-NMR. Figure 5 shows the spectra corresponding to different steps of the polymerization reaction. The initial spectrum, which

corresponds to the time when IPDI was added, is characterized by the strong band at 2260 cm^{-1} attributed to the stretching vibration of isocyanate groups, the band at 1100 cm^{-1}, which corresponds to the C-O-C stretching vibration of PPG, and the band at 1710 cm^{-1}, which corresponds to the urethane carbonyl stretching vibration. In addition, the shoulder at 1776 cm^{-1} is assigned to the DA adduct, which corresponds to the non-conjugated carbonyl stretching vibration. As the reaction progresses the band corresponding to isocyanate groups decreases and the bands due to Amide I (1710 cm^{-1}) and Amide II (1550 cm^{-1}) of the urethane groups increase. Finally, in the last spectrum, there is no isocyanate band, which indicates that the reaction has taken place properly.

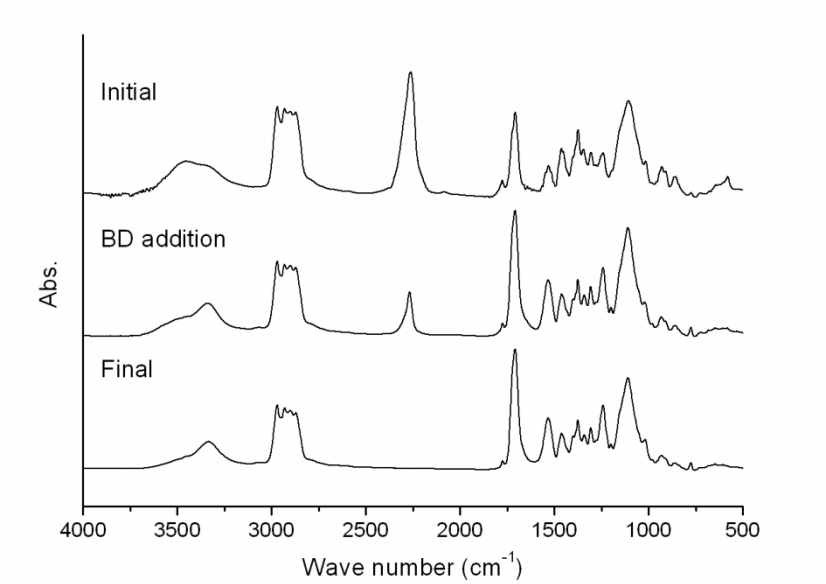

Figure 5 FTIR spectra at different reaction steps of PUDA12 sample.

Figure 6 shows the ^{1}H-NMR of the final product and the band assignment.

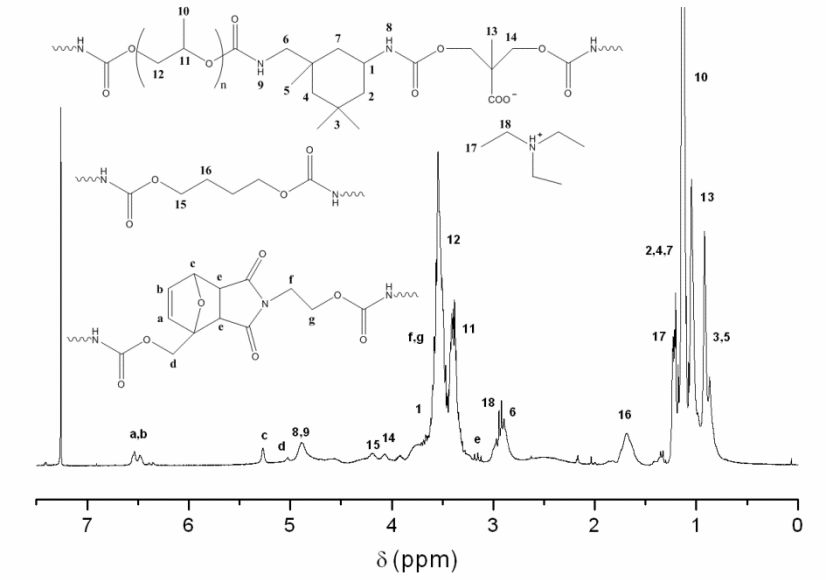

Figure 6 ^{1}H NMR spectrum and line assignment for PUDA12.

The structure of the polymer was confirmed by ^{1}H-NMR spectroscopy (Figure 6).

Water dispersions

The particle size was measured by DLS. PUMA polymers presented strange behaviour in the dispersion stability. After the water dispersion process, the dispersion was instable and became stable after 12 hours. In order to clarify the origin of this behaviour ^{1}H-NMR spectrum was carried out after dispersion took place (Figure 7). The appearance of a double pair of signals around 6-6.5 ppm, not present in the non-dispersed polymer spectrum, reveals that the polymer structure changed after the dispersion process. These signals can be explained by the maleimide ring opening (Scheme 3) that can occur when the maleimide is in basic environment [47], the environment used to stabilize the polyurethane dispersions. The new double bond formed by maleimide hydrolysis is responsible for the signals around 6-6.5 ppm. Therefore, it can be seen that the maleimide is hydrolyzed in the dispersion process. This hydrolysis side reaction prevented the use of these polymers as the DA adduct is destroyed during the dispersion process.

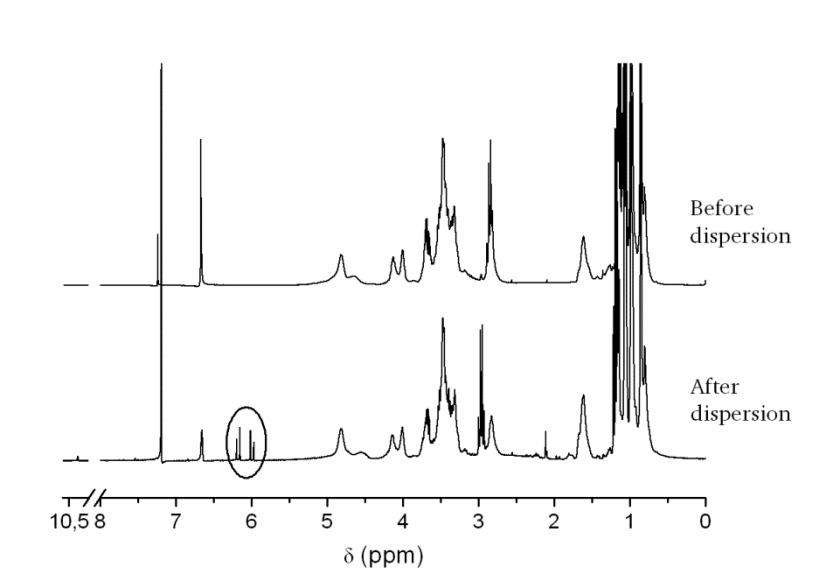

Figure 7 ^{1}H-NMR spectra for PUMA10 before and after dispersion.

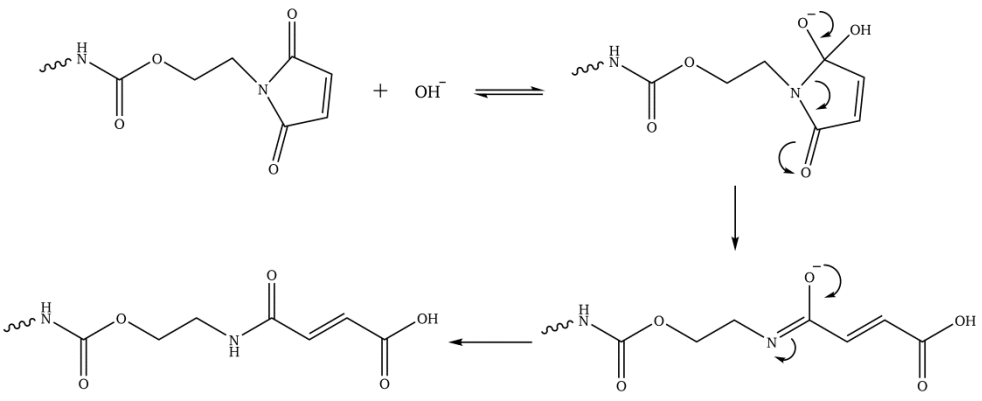

Scheme 3 The mechanism of PUDA polymer chain ends maleimide group hydrolysis.

However, the dispersions obtained from PUFAM and PUDA systems were stable. The particle size of these dispersions changed with the stimuli-responsive monomer percentage. As can be seen in Table 4, in both systems the particle size decreases with the stimuli-responsive concentration, indicating that in both cases the stimuli-responsive compound increases the dispersion capacity of the polymer.

Polymer	PUFAM5	PUFAM7	PUFAM10	PUDA6	PUDA9	PUDA12
Dp (nm)	90 ± 3	60 ± 2	57 ± 2	80 ± 1	56 ± 1	46 ± 4

Table 4 Particle size of PUFAM and PUDA polymers.

Characterization of the Diels-Alder reaction by FTIR

- *Furan end capped polyurethanes (PUFAM)*

In order to induce the Diels-Alder reaction a maleimide compound must be added to the furan end capped systems (PUFAM). However, as described in the previous paragraphs maleimide is hydrolyzed in basic medium thus avoiding direct addition to the dispersion. In order to eliminate this reaction some attempts were made to decrease the pH of the PUMA dispersions but they were destabilized, preventing the use of the PUMA system. Therefore, a low molecular weight bismaleimide was selected to introduce into the PUFAM systems. Consequently, different dispersions of PUFAM were dried and using acetone as solvent the stoichiometric amount of bismaleimide was added. The reaction was followed in-situ by FTIR at 60 ^{o}C, using a heating accessory. Figure 8 shows the spectra corresponding to different reaction times. As the reaction progresses, the bands assigned to the bismaleimide o.o.p. bending vibrations of the double bonds decrease in intensity (830 cm^{-1} and 690 cm^{-1}). This indicates that the Diels-Alder reaction occurs, since in this reaction the double bond of bismaleimide is lost. In addition, a small shoulder at about 1780 cm^{-1} appears. This band is characteristic of the DA adduct which corresponds to the non-conjugated carbonyl stretching vibration [48–50].

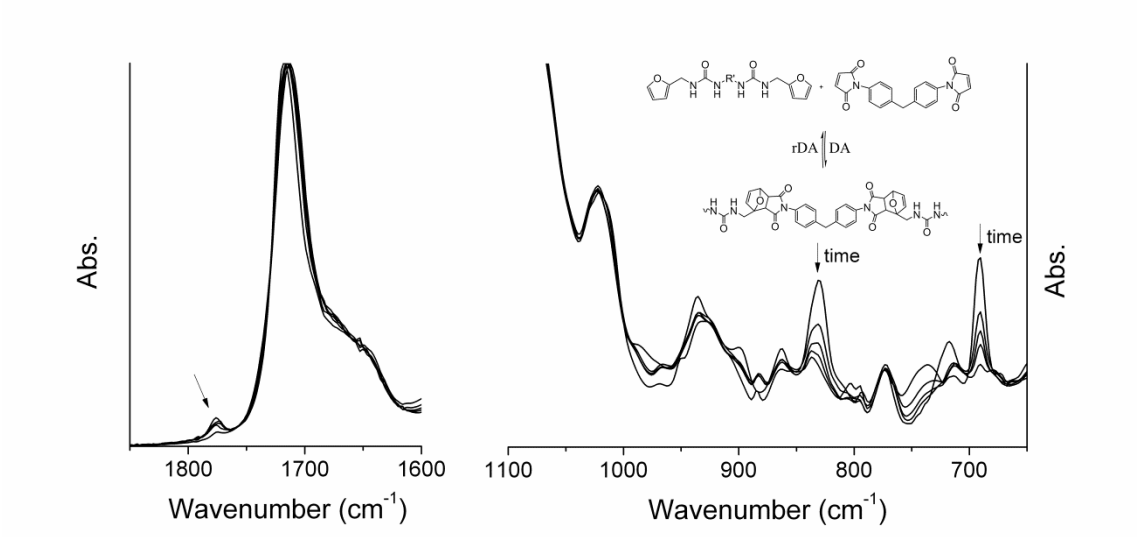

Figure 8 FTIR spectra as a function of time at 60 ^{o}C for PUFAM10.

From the evolution of the absorbance of the band at 830 cm^{-1} as a function of the reaction time, the conversion (α) was calculated according to eq (1).

$$\alpha = 1 - \frac{A_t}{A_{t_0}} \qquad (1)$$

Where A_{t0} and A_t are the normalized absorptions at t=0 and t of the band at 830 cm^{-1} with respect to the stretching vibrations of aliphatic groups (2980-2800 cm^{-1}).

In order to determine the influence of temperature on the conversion, the DA reaction was studied at several temperatures [18]. Figure 9 shows the results for the PUFAM10 sample. As can be seen, the reaction conversion increases sharply in the first 100 min, and then slows down until maximum conversion is reached. In addition, although the reaction rate at 60 ^oC and 80 ^oC are similar, the maximum conversion achieved at 80 ^oC is lower. This phenomenon indicates that the retro Diels-Alder reaction starts dominating at 80 ^oC [13]. Therefore, 80 ^oC is not a suitable temperature for Diels-Alder reaction, because the reaction does not achieve high conversions. Similar results were obtained in literature by UV spectroscopy [13]. Consequently, 60 ^oC was selected as the optimum temperature to perform the Diels-Alder reaction.

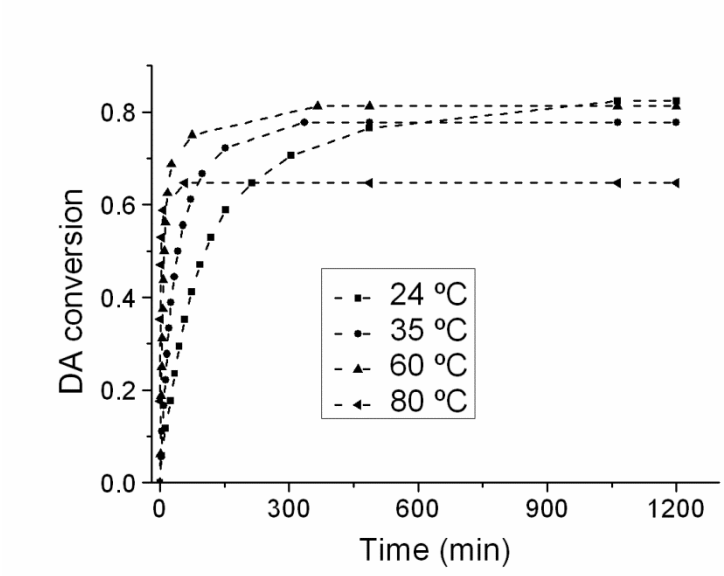

Figure 9 Conversion degree as a function of time for PUFAM10.

It is well known that the Diels-Alder reaction is thermo reversible. According to different authors [9,13] when the DA adduct is heated at 100 ^oC the retro Diels-Alder reaction can achieve equilibrium in about 60 minutes and less time at higher temperatures. According to this and taking into account previous results obtained in our group [18], 120 ^oC was selected as the temperature at which to perform the retro Diels-Alder reaction. For this aim the PUFAM10-DA sample was heated at 120 ^oC and FTIR spectra were recorded at different times (Figure 10). As can be seen, the bands assigned to the bismaleimide o.o.p. bending vibrations of the double bonds increase in intensity (830 cm^{-1} and 690 cm^{-1}), due to the formation of bismaleimide. These results confirm that the reaction is reversible as upon heating the DA adduct is opened regenerating the original compounds. From these measurements the DA

conversion was calculated. Figure 10 shows the calculated Diels-Alder conversion as a function of retro Diels-Alder reaction time. During the reaction the Diels-Alder conversion decreases. Additionally, it can be seen that the retro Diels-Alder reaction occurs faster than the Diels-Alder reaction, as in 15 minutes a constant DA conversion is reached. However, it should be pointed out that in the retro Diels-Alder reaction the DA conversion to zero value is not reached. This indicates that the retro Diels-Alder reaction is not total, which means that all the DA adduct formed in the Diels-Alder reaction does not return to furan and bismaleimide compounds. The same behaviour has been observed in literature [13].

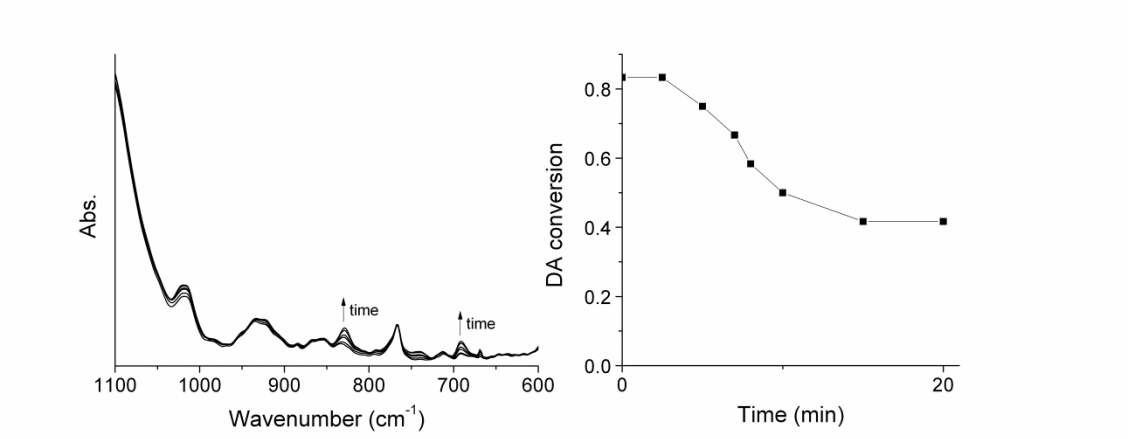

Figure 10 FTIR spectra and DA conversion as a function of rDA reaction time for PUFAM10.

- DA adduct containing polyurethanes (PUDA)

As the DA adduct is already formed in PUDA polymers only the retro Diels-Alder reaction was followed. Figure 11 shows FTIR spectra at different times for one of the samples. As can be seen, the bands assigned to the maleimide o.o.p. bending vibrations of the double bonds increased in intensity (830 cm^{-1} and 690 cm^{-1}), owing to the formation of maleimide that occurs as a consequence of the retro Diels-Alder reaction. Unfortunately, in this case the DA conversion cannot be calculated, as the area at 830 cm^{-1} of the sample without DA adduct is unknown. However, with this result the time to perform the retro Diels-Alder reaction can be measured, as after 10 minutes the area of the band does not change.

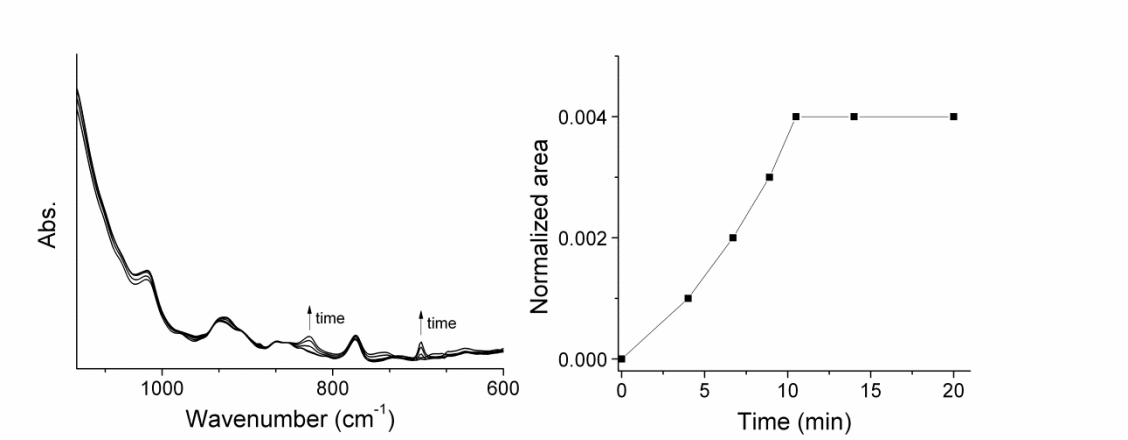

Figure 11 FTIR spectra and the normalized area of the band at 830 cm^{-1} as a function of time for PUDA12.

Characterization of Diels-Alder reaction by ^{1}H-NMR spectroscopy

In order to follow the Diels-Alder reaction between PUFAM and bismaleimide, the polymer and bismaleimide (equivalent mol ratio) were mixed in acetone. The solution was casted onto a Teflon mould, which was heated at 60 ^{o}C. Different spectra were carried out at different times. As can be seen in Figure 12, the intensity of the signals corresponding to furan and maleimide protons (a, b, c and e) decreases as the Diels-Alder reaction takes place, and new signals (a',b' and c') assignable to DA adduct appear [49,51].

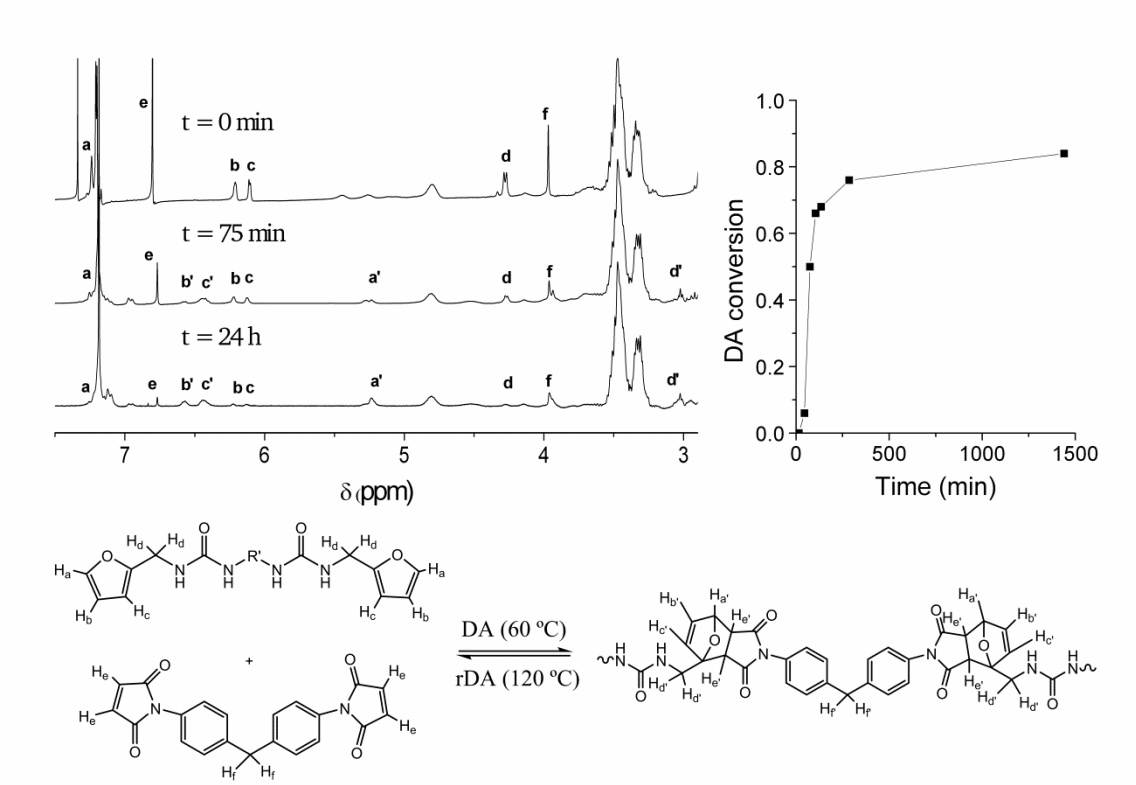

Figure 12 ^{1}H-NMR evolution at different reaction times at 60 ^{o}C, the calculated conversion and structural assignment for PUFAM10 sample.

The ^{1}H-NMR spectra changes allow a quantitative analysis of the Diels-Alder reaction. Thus, the signals assigned to furan protons (b, c) and the signals assigned to DA adduct (b ', c') were used to calculate the Diels-Alder reaction conversion, according to eq. (2).

$$\text{Conversion} = \frac{A_{b'+c'}}{A_{b'+c'} + A_{b+c}} \qquad (2)$$

As can be seen, the conversion achieved in the reaction is around 85 %. It is worth pointing out that a similar result has been achieved using infrared spectroscopy (Figure 9). This indicates that both techniques are useful in following the reaction.

NMR spectroscopy can also be used to study the retro Diels-Alder reaction in both systems, due to the reversibility of the reaction. Therefore, in order to induce the retro Diels-Alder

reaction the samples were heated at 120 °C for 20 minutes in an oven and then the ^{1}H-NMR spectra were performed. Figure 13 shows the spectrum before and after the retro Diels-Alder for both systems. As can be seen, the signals assigned to furan protons (b, c) and DA adduct protons (b', c') change intensity, due to the retro Diels-Alder reaction. All these results show that at 120 °C the retro Diels-Alder reaction occurs in both types of samples. However, as can be seen, the retro Diels-Alder reaction is not total as the signal assigned to DA adduct protons (b', c') do not disappear completely. These results are in good agreement with those obtained by FTIR.

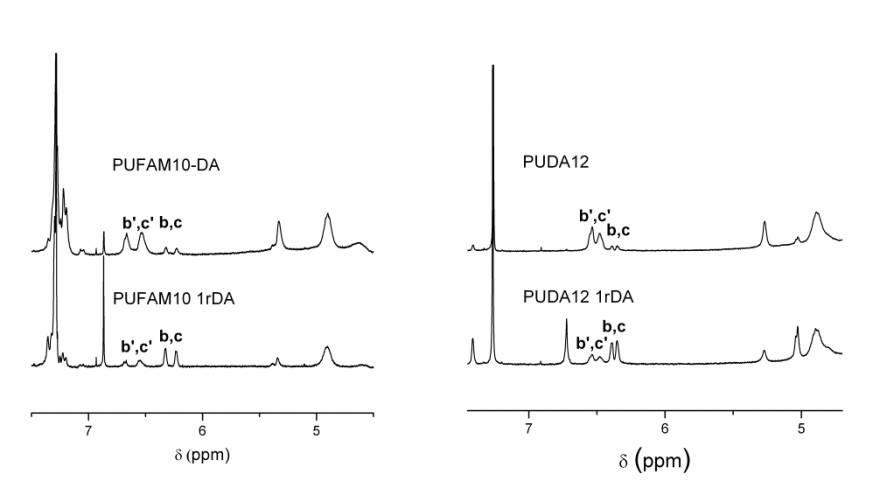

Figure 13 PUFAM10-DA, PUFAM10 1rDA, PUDA12 and PUDA 1rDA ^{1}H-NMR spectrum.

Thermal reversibility study

In order to study the thermal reversibility of the samples, different heating treatments were performed, to produce retro Diels-Alder and Diels-Alder reactions (Scheme 4). After each cycle ^{1}H-NMR spectra were carried out and the DA conversion was calculated. This treatment was performed for all samples of both systems and the results are shown in Figure 14 and Figure 15.

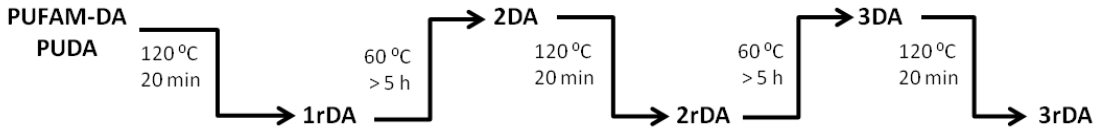

Scheme 4 Different heating treatments for testing the thermal reversibility of PUFAM-DA and PUDA.

As can be seen in Figure 14, for the furan end capped polymers, regardless of the furan content all samples reach the same initial DA conversion, which is about 85 %. When the retro Diels-Alder reaction occurs, the DA conversion value decreases till 30 %. Both conversion data remain practically constant no matter the number of DA and rDA cycles. This behaviour indicates the good reversibility of the reaction.

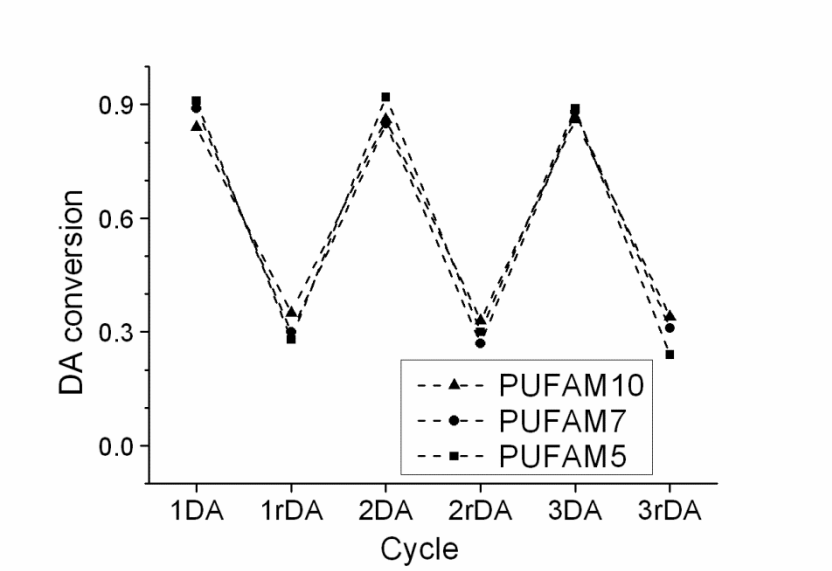

Figure 14 Evolution of DA conversion as a function of cycle treatment for PUFAM samples.

As for the behaviour of the DA adduct containing polyurethanes (PUDA), all the samples show a initial conversion of about 80 % (Figure 15). By means of the retro Diels-Alder reaction the conversion decreases to around 30 %. However, in these polymers in the second and third DA cycles, the Diels-Alder reaction does not achieve the initial conversion. This indicates that efficiency is lost in the different cycles, especially from the first cycle to the others.

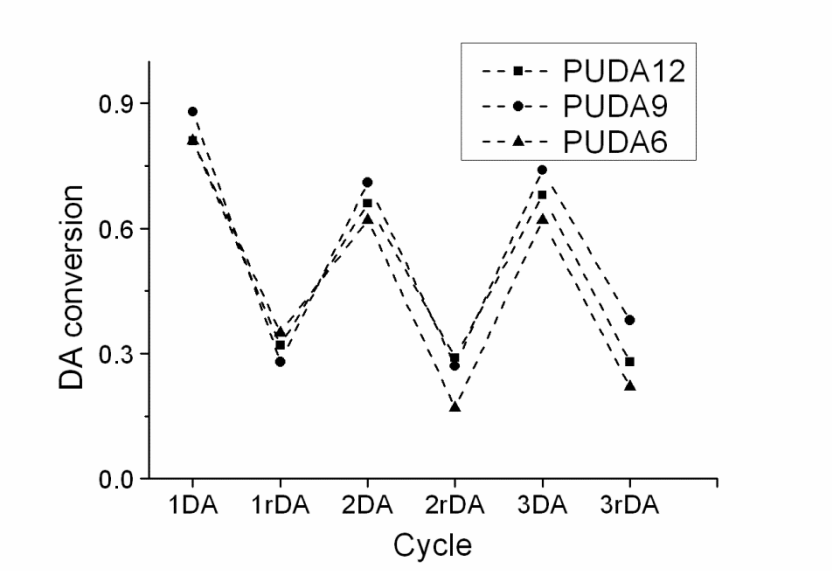

Figure 15 Evolution of DA conversion as a function of cycle treatment for PUDA samples.

When both systems (PUFAM vs PUDA) are compared, it should be pointed out that in both, the Diels-Alder and retro Diels Alder reactions occur in a proper way. However, there is a loss of efficiency in the PUDA system which does not exist in the PUFAM one. This behaviour can be related to the differences in the viscosity and/or the hydrogen bonding abilities of both systems.

With respect to viscosity as it is shown in next section (Figure 19 and Figure 20), PUFAM systems show higher viscosity than PUDA systems. A slight increase in the DA reaction rate constant has been related in literature in the frame of a possible cage effect of the solvent [52]. In as similar way, the behavior observed in our work for the PUFAM system can be related to the high viscosity which increases the cage effect, providing higher DA conversions.

Regarding the hydrogen bonding abilities of both systems it should be considered that the introduction of DA moieties in PUFAM and PUDA system was made via urea and urethane groups respectively. Thus, the hydrogen bonding abilities of both systems can be different. In order to study this possible effect, theoretical physicochemical analysis of non-covalent interactions before retro Diels-Alder reaction takes place were done using NCIPLOT software [46].

The Non-Covalent Index [45] topological analysis give the possibility to visually observe the nature, intensity and the spatial distribution of the electron density in models of PUFAM-BMI and PUDA polymers. According to these calculations, PUDA system is able to form two different complexes ready to undertake Diels-Alder reaction. One of these complexes presents a hydrogen bond between the urethane groups of PUDA (Figure 16b), while the other (3 kcal/mol more stable) shows an hydrogen bond between the urethane of PUDA and the maleimide carbonyl (Figure 16c). On the other hand, PUFAM-BMI model presents a hydrogen bond between the further amine group of the furan ring and the maleimide carbonyl (Figure 16a). Regarding the intensity of the hydrogen bonds, PUDA system shows stronger intensity (bluish color in the image) than PUFAM-BMI system (green color). Moreover, this is in good agreement with the found hydrogen bond distances, 1.99 A and 2.3 A respectively.

As a conclusion, this analysis has shown that PUDA systems are able to form stronger non covalent interactions than PUFAM system. Thus, the higher efficiency of the DA reaction observed in the latter cannot be attributed to hydrogen bonding abilities. Taking this into account, the higher efficiency can be explained by the cage effect originated by the higher sample viscosity as described in previous paragraph.

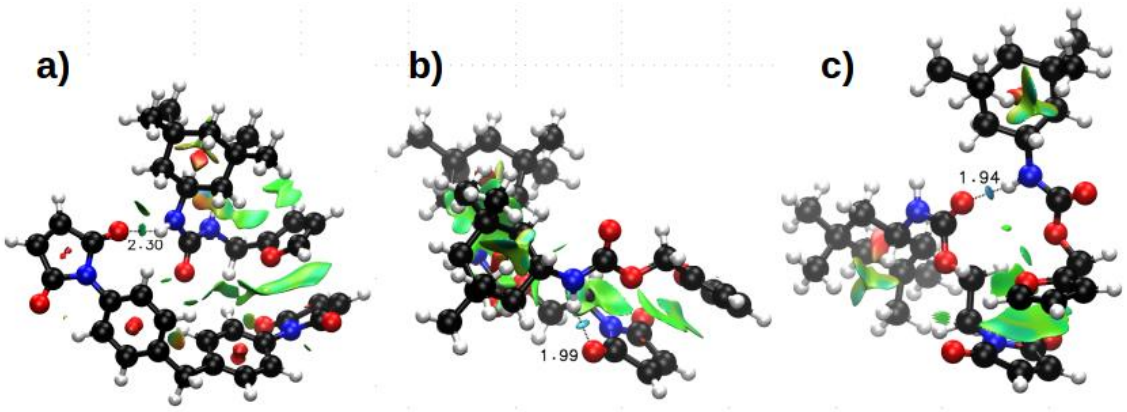

Figure 16 Representation of the non covalent interactions for PUFAM-BMI (a) and PUDA (b,c) models. Blue color represents attractive interactions, green color represents weak interactions and red color means repulsive interactions.

DSC Study

The thermal reversibility was also studied by DSC analysis [53]. For this aim different DSC thermograms were obtained after treating the samples under the procedure described in Scheme 4. Figure 17 shows an example for each system. As can be seen, PUFAM10-DA and PUDA12 samples, in addition to the Tg transition, show an endothermic peak at about 120 ^{o}C that disappears in a second scan. This result confirms the fact that the retro DA reaction is responsible for the endothermic transition [50,54]. In addition, as the endothermic peak re-appeared in the second and third DA cycles it can be concluded that the samples have good thermal reversibility. However, whereas the enthalpy of the process for PUFAM10 polymer is independent of the number of cycles, for PUDA12 sample the enthalpy decreases slightly. This fact indicates that in this system there is an efficiency loss in the different cycles, especially from the first cycle to the next. This result confirms the data obtained by NMR and is due to the lower viscosity of this system, as concluded in previous section. The DSC thermograms of the rest of the samples (data not shown) give rise to similar results confirming the reversibility of the Diels-Alder reaction in all samples.

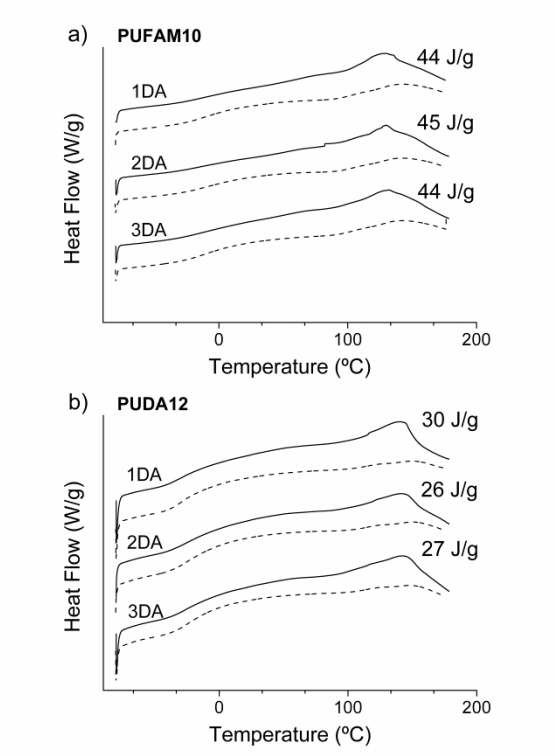

Figure 17 DSC thermograms for PUFAM10 and PUDA12 samples after each heating cycles (continuous line for 1st run and dashed line for 2nd run).

Physical response characterization

From the previous results it is clear that the retro Diels-Alder reaction which occurs at 120 ^{o}C results in the disconnection between furan and maleimide group, while the DA adduct is regenerated at lower temperatures (Scheme 5). This fact causes important changes in the molecular weight of the polymer which can also be used to study the thermo-reversibility of the reaction [12].

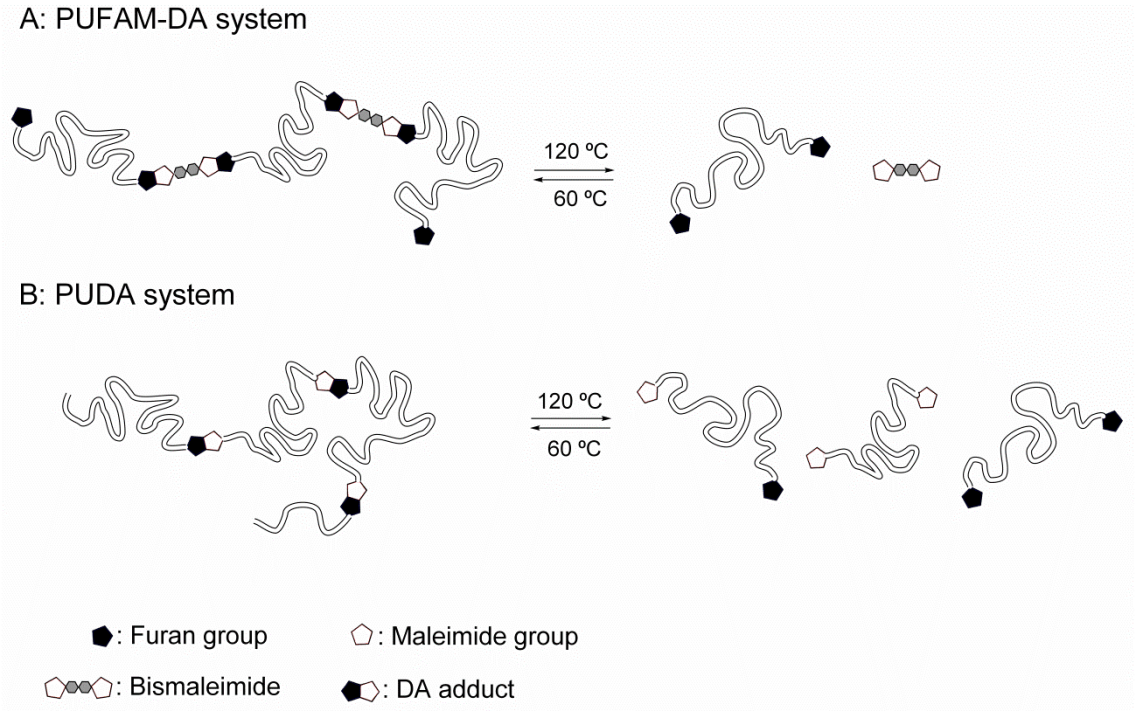

Scheme 5 Schematic representation of the polymer chains response for PUFAM-DA system (a) and PUDA system (b).

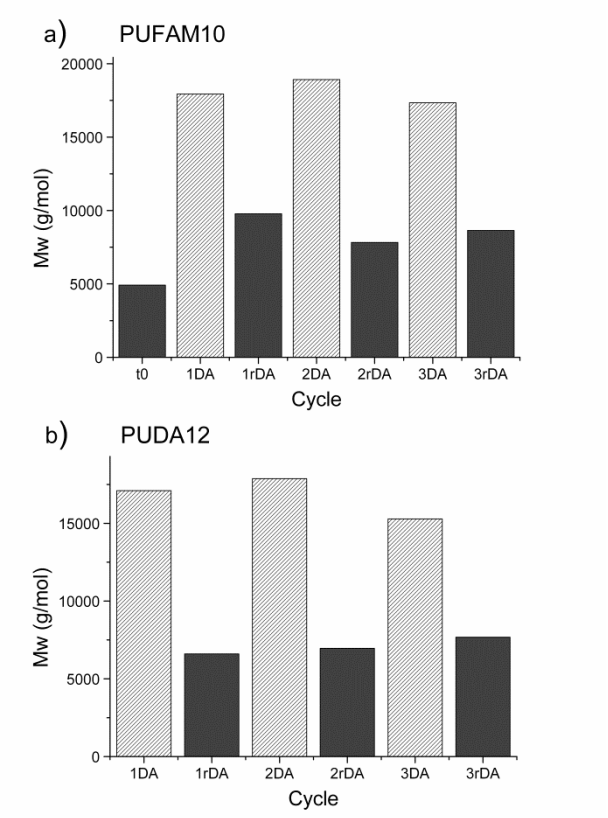

Figure 18 Molecular weight (Mw) of PUFAM10 (a) and PUDA12 (b) samples after each heating cycles.

For this purpose, thermal cycles (120 ºC / 60 ºC) were applied to the sample (Scheme 4), and after each cycle the molecular weight of the polymer was calculated by Size Exclusion Chromatography (SEC). As can be seen in Figure 18, in both systems Mw decreases when the retro DA takes place and increases when the DA reaction occurs. Moreover, this behaviour is repeated in the second and third Diels-Alder and retro Diels-Alder cycles indicating the good thermal reversibility of PUFAM and PUDA polymers.

Furthermore, the physical response to temperature can also be studied by rheological measurements, as the material viscosity is clearly affected by the changes in the polymer chain length. Therefore, the rheological behaviour was analyzed at Diels-Alder and retro Diels-Alder reaction temperatures, 60 ºC and 120 ºC, respectively. In addition, in order to demonstrate that the results obtained are not only because of the influence of the temperature, a polyurethane model (PU) was studied without the stimuli-responsive compound. As the above mentioned results show that the Diels-Alder and retro Diels-Alder reactions take place properly in all samples, measurements were only done for one sample of each system.

Figure 19 shows PU and PUFAM7-DA viscosities as a function of time at different temperatures. When the PUFAM7-DA sample is heated at 120 ºC (1. Cycle), the viscosity decreases with time. This indicates that the retro Diels-Alder reaction occurs. As mentioned, due to this reaction the polymer chain is broken, decreasing the molecular weight and thus decreasing the viscosity of the sample. Afterwards, the sample is cooled to 60 ºC. The samples at this temperature have a higher viscosity due to the effect of the temperature (usually the viscosity value at low temperature is higher). However, as can be seen, the viscosity of this sample increases over time at 60 ºC, which indicates that the polymer chains are growing again due to the Diels-Alder reaction. On the contrary, the viscosity of the PU sample without the DA adduct does not exhibit changes with time. This fact indicates that the viscosity changes observed in the stimuli-responsive polymers are due to the molecular weight changes induced by the Diels-Alder and retro Diels-Alder reaction.

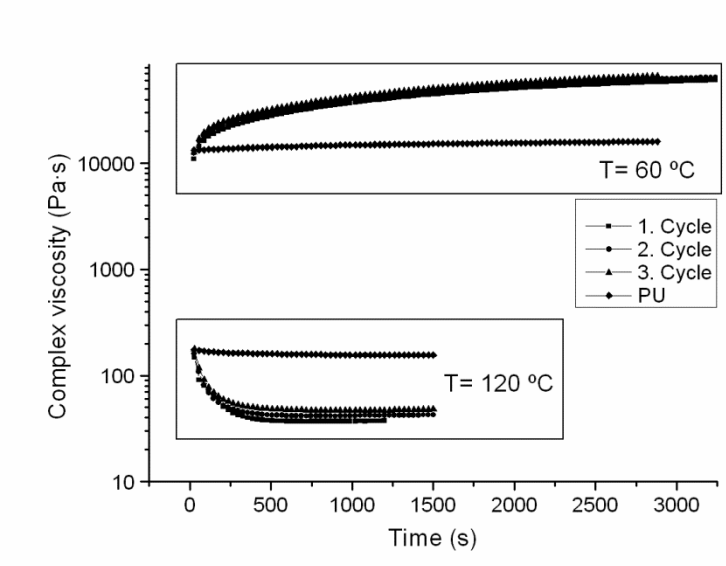

Figure 19 Complex viscosity as a function of time at different temperatures for PUFAM7 and PU samples.

Figure 20 shows the viscosity of the PUDA9 sample as a function of time at 60 ºC and 120 ºC. As expected, this polymer shows the same behaviour as the PUFAM7 polymer. Thus, when the sample is heated at 120 ºC the viscosity decreases because of the retro Diels-Alder reaction, while when it is heated at 60 ºC the Diels-Alder reaction increases the viscosity. This behaviour is independent of the number of cycles showing the good thermal reversibility of the systems.

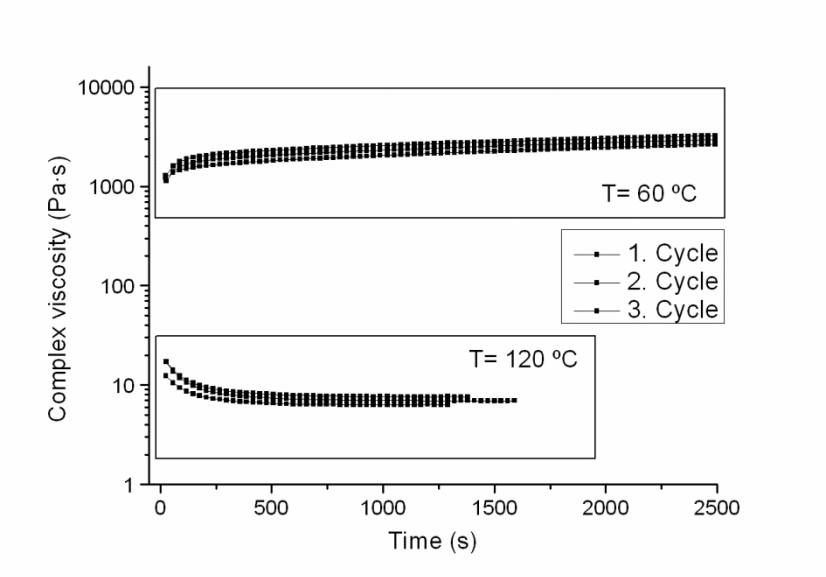

Figure 20 Complex viscosity as a function of time at different temperatures for PUDA9 sample.

Therefore, these results show that the retro Diels-Alder reaction considerably reduces the viscosity of the system. This fact can be of great interest when developing self-healing materials as a lower viscosity will favour the crack filling during the healing process.

Conclusion

Two different strategies were used to obtain stimuli-responsive waterborne polyurethanes. The first one based on mixing furan and maleimide end capped polyurethane dispersions was not very appropriate because of the maleimide hydrolysis that occur at basic pH. Nevertheless, by drying the furan capped dispersion and mixing with maleimide compound it was possible to demonstrate that Diels-Alder and retro Diels-Alder reactions take place when the samples are exposed to different temperatures.

The second strategy based on introducing the DA adduct in the polymer structure using a modified diol, allows the obtaining of novel one pot stable stimuli-responsive waterborne polyurethane dispersions. In this system, the temperature induced Diels-Alder and retro Diels-Alder reactions, studied by FTIR, NMR and DSC, give rise to molecular weight variations (measured by SEC) that produced important changes in the viscosity. These new temperature responsive linear waterborne polyurethanes can be of great interest in the development of functional and sustainable coatings.

Acknowledgements

The authors acknowledge the University of the Basque Country UPV/EHU (UFI 11/56) and the Basque Government (IT618-13) for the funding received to develop this work. Technical and human support provided by Macro-behaviour-Mesostructure Nanotechnology and NMR SGIker Services of UPV/EHU is also gratefully acknowledged.

References

[1] P. Uhlmann, R. Frenzel, B. Voit, U. Mock, B. Szyszka, B. Schmidt, D. Ondratschek, J. Gochermann, K. Roths, Research agenda surface technology: Future demands for research in the field of coatings materials, Prog. Org. Coatings. 58 (2007) 122–126.

[2] Y. Yang, M.W. Urban, Self-healing polymeric materials, Chem. Soc. Rev. 42 (2013) 7446–7467.

[3] S.K. Ghosh, Self-healing materials: Fundamentals, Design Strategies and Applications, WILEY-VCH Verlag & Co. KGaA, Weinheim, Germany, 2009.

[4] V.K. Thakur, M.R. Kessler, Self-healing polymer nanocomposite materials: A review, Polymer. 69 (2015) 369–383.

[5] K.M. Herbert, S. Schrettl, S.J. Rowan, C. Weder, 50th Anniversary Perspective: Solid-State Multistimuli, Multiresponsive Polymeric Materials, Macromolecules. 50 (2017) 8845–8870.

[6] N.K. Guimard, K.K. Oehlenschlaeger, J. Zhou, S. Hilf, F.G. Schmidt, C. Barner-Kowollik, Current trends in the field of self-healing materials, Macromol. Chem. Phys. 213 (2012) 131–143.

[7] D.Y. Wu, S. Meure, D. Solomon, Self-healing polymeric materials: A review of recent developments, Prog. Polym. Sci. 33 (2008) 479–522.

[8] A. Gandini, S. Boufi, H. Laita, The application of the Diels-Alder reaction to polymers bearing furan moieties. 1. Reactions with maleimides, Eur. Polym. J. 33 (1997) 1203–1211.

[9] A. Gandini, The furan/maleimide Diels–Alder reaction: A versatile click–unclick tool in macromolecular synthesis, Prog. Polym. Sci. 38 (2013) 1–29.

[10] G. Zhang, Q. Zhao, L. Yang, W. Zou, X. Xi, T. Xie, Exploring Dynamic Equilibrium of Diels-Alder Reaction for Solid State Plasticity in Remoldable Shape Memory Polymer Network, ACS Macro Lett. 5 (2016) 805–808.

[11] Y.L. Liu, T.W. Chuo, Self-healing polymers based on thermally reversible Diels–Alder chemistry, Polym. Chem. 4 (2013) 2194–2205.

[12] P. Du, X. Liu, Z. Zheng, X. Wang, T. Joncheray, Y. Zhang, Synthesis and characterization of linear self-healing polyurethane based on thermally reversible Diels–Alder reaction, RSC Adv. 3 (2013) 15475–15482.

[13] X. Liu, P. Du, L. Liu, Z. Zheng, X. Wang, T. Joncheray, Y. Zhang, Kinetic study of Diels–Alder reaction involving in maleimide–furan compounds and linear polyurethane, Polym. Bull. 70 (2013) 2319–2335.

[14] P. Du, H. Jia, Q. Chen, Z. Zheng, X. Wang, D. Chen, Slightly crosslinked polyurethane with Diels-Alder adducts from trimethylolpropane, J. Appl. Polym. Sci. 133 (2016) 1–8.

[15] P. Du, M. Wu, X. Liu, Z. Zheng, X. Wang, T. Joncheray, Y. Zhang, Diels-Alder-based crosslinked self-healing polyurethane/urea from polymeric methylene diphenyl diisocyanate, J. Appl. Polym. Sci. 131 (2014) 40234–40241.

[16] Y. Wei, X. Ma, The self-healing cross-linked polyurethane by Diels-Alder polymerization, Adv. Polym. Technol. (2017) 1–7.

[17] K. Ishida, V. Weibel, N. Yoshie, Substituent effect on structure and physical properties of semicrystalline Diels-Alder network polymers, Polymer. 52 (2011) 2877–2882.

[18] L. Irusta, M.J. Fernández-Berridi, J. Aizpurua, Polyurethanes based on isophorone diisocyanate trimer and polypropylene glycol crosslinked by thermal reversible diels alder reactions, J. Appl. Polym. Sci. 134 (2017) 1–9.

[19] S. Yu, R. Zhang, Q. Wu, T. Chen, P. Sun, Bio-Inspired High-Performance and Recyclable Cross-Linked Polymers, Adv. Mater. 25 (2013) 4912–4917.

[20] C. Varganici, O. Ursache, C. Gaina, V. Gaina, D. Rosu, B.C. Simionescu, Synthesis and Characterization of a New Thermoreversible Polyurethane Network, Ind. Eng. Chem. Res. 52 (2013) 5287–5295.

[21] R. Zhang, S. Yu, S. Chen, Q. Wu, T. Chen, P. Sun, B. Li, D. Ding, Reversible cross-linking, microdomain structure, and heterogeneous dynamics in thermally reversible cross-linked polyurethane as revealed by solid-state nmr, J. Phys. Chem. B. 118 (2014) 1126–1137.

[22] C. Lin, D. Sheng, X. Liu, S. Xu, F. Ji, L. Dong, Y. Zhou, Y. Yang, A self-healable nanocomposite based on dual-crosslinked Graphene Oxide/Polyurethane, Polym. 127 (2017) 241–250.

[23] S. Chen, F. Wang, Y. Peng, T. Chen, Q. Wu, P. Sun, A Single Molecular Diels – Alder Crosslinker for Achieving Recyclable Cross-Linked Polymers, Macromol. Rapid Commun. 36 (2015) 1687–1692.

[24] X. Ke, H. Liang, L. Xiong, S. Huang, M. Zhu, Synthesis, curing process and thermal reversible mechanism of UV curable polyurethane based on Diels-Alder structure, Prog. Org. Coatings. 100 (2016) 63–69.

[25] B. Willocq, F. Khelifa, J. Brancart, G. Van Assche, P. Dubois, J.M. Raquez, One-component Diels–Alder based polyurethanes: a unique way to self-heal, RSC Adv. 7 (2017) 48047–48053.

[26] E. Dolci, V. Froidevaux, G. Michaud, F. Simon, R. Auvergne, S. Fouquay, S. Caillol, Thermoresponsive crosslinked isocyanate-free polyurethanes by Diels-Alder polymerization, J. Appl. Polym. Sci. 134 (2017) 1–11.

[27] C. Lakatos, K. Czifrák, J. Karger-Kocsis, L. Daróczi, M. Zsuga, S. Kéki, Shape memory crosslinked polyurethanes containing thermoreversible Diels-Alder couplings, J. Appl. Polym. Sci. 133 (2016) 1–9.

[28] Y. Heo, H.A. Sodano, Self-healing polyurethanes with shape recovery, Adv. Funct. Mater. 24 (2014) 5261–5268.

[29] K. Zheng, Y. Tian, M. Fan, J. Zhang, J. Cheng, Recyclable, shape-memory, and self-healing soy oil-based polyurethane crosslinked by a thermoreversible Diels–Alder reaction, J. Appl. Polym. Sci. 135 (2018) 1–10.

[30] C. Lakatos, K. Czifrák, R. Papp, J. Karger-Kocsis, M. Zsuga, S. Kéki, Segmented linear shape memory polyurethanes with thermoreversible diels-alder coupling: Effects of polycaprolactone molecular weight and diisocyanate type, Express Polym. Lett. 10 (2016) 324–336.

[31] W. Chen, Y. Zhou, Y. Li, J. Sun, X. Pan, Q. Yu, N. Zhou, Z. Zhang, X. Zhu, Shape-memory and self-healing polyurethanes based on cyclic poly(ε-caprolactone), Polym. Chem. 7 (2016) 6789–6797.

[32] G. Rivero, L.T.T. Nguyen, X.K.D. Hillewaere, F.E. Du Prez, One-pot thermo-remendable shape memory polyurethanes, Macromolecules. 47 (2014) 2010–2018.

[33] R.H. Aguirresarobe, L. Martin, N. Aramburu, L. Irusta, M.J. Fernandez-Berridi, Coumarin based light responsive healable waterborne polyurethanes, Prog. Org. Coatings. 99 (2016) 314–321.

[34] R.H. Aguirresarobe, L. Martin, M.J. Fernandez-Berridi, L. Irusta, Autonomic healable waterborne organic-inorganic polyurethane hybrids based on aromatic disulfide moieties, Express Polym. Lett. 11 (2017) 266–277.

[35] J. Luna, M. Lansalot, H. Sardon, L. Irusta, M.J. Fernández-Berridi, Waterborne Polyurethane Dispersions Obtained by the Acetone Process: A Study of Colloidal Features, J. Appl. Polym. Sci. 120 (2011) 2054–2062.

[36] A.K. Nanda, D. Wicks, The influence of the ionic concentration, concentration of the polymer, degree of neutralization and chain extension on aqueous polyurethane dispersions prepared by the acetone process, Polymer. 47 (2006) 1805–1811.

[37] V. Garcia-Pacios, V. Costa, M. Colera, J.M. Martin-Martinez, Waterborne polyurethane dispersions obtained with polycarbonate of hexanediol intended for use as coatings, Prog. Org. Coatings. 71 (2011) 136–146.

[38] N. Salewska, M.J. Milewska, Efficient Method for the Synthesis of Functionalized Basic Maleimides, J. Heterocycl. Chem. 51 (2014) 999–1003.

[39] V. García-Pacios, Y. Iwata, M. Colera, J.M. Martín-Martínez, Influence of the solids content on the properties of waterborne polyurethane dispersions obtained with polycarbonate of hexanediol, Int. J. Adhes. Adhes. 31 (2011) 787–794.

[40] M.J. Frisch, G.W. Trucks, H.B. Schlegel, G.E. Scuseria, M.A. Robb, J.R. Cheeseman, G. Scalmani, V. Barone, B. Mennucci, G.A. Petersson, H. Nakatsuji, M. Caricato, X. Li, H.P. Hratchian, A.F. Izmaylov, J. Bloino, G. Zheng, J.L. Sonnenberg, M. Hada, M. Ehara, K. Toyota, R. Fukuda, J. Hasegawa, M. Ishida, T. Nakajima, Y. Honda, O. Kitao, H. Nakai, T. Vreven, J. J. A. Montgomery, J.E. Peralta, F. Ogliaro, M. Bearpark, J.J. Heyd, E. Brothers, K.N. Kudin, V.N. Staroverov, R. Kobayashi, J. Normand, K. Raghavachari, A. Rendell, J.C. Burant, S.S. Iyengar, J. Tomasi, M. Cossi, N. Rega, J.M. Millam, M. Klene, J.E. Knox, J.B. Cross, V. Bakken, C. Adamo, J. Jaramillo, R. Gomperts, R.E. Stratmann, O. Yazyev, A.J. Austin, R. Cammi, C. Pomelli, J.W. Ochterski, R.L. Martin, K. Morokuma, V.G. Zakrzewski, G.A. Voth, P. Salvador, J.J. Dannenberg, S. Dapprich, A.D. Daniels, O. Farkas, J.B. Foresman, J. V. Ortiz, J. Cioslowski, D.J. Fox, Gaussian 09, Revision A.02, (2009).

[41] Y. Zhao, D.G. Truhlar, The M06 suite of density functionals for main group thermochemistry, thermochemical kinetics, noncovalent interactions, excited states, and transition elements: Two new functionals and systematic testing of four M06-class functionals and 12 other function, Theor. Chem. Acc. 120 (2008) 215–241.

[42] T.H. Dunning, Gaussian basis sets for use in correlated molecular calculations. I. The atoms boron through neon and hydrogen, J. Chem. Phys. 90 (1989) 1007–1023.

[43] R.A. Kendall, T.H. Dunning, R.J. Harrison, Electron affinities of the first-row atoms revisited. Systematic basis sets and wave functions, J. Chem. Phys. 96 (1992) 6796–6806.

[44] R.K. Singh, T. Tsuneda, Reaction energetics on long-range corrected density functional theory: Diels-Alder reactions, J. Comput. Chem. 34 (2013) 379–386.

[45] E.R. Johnson, S. Keinan, P. Mori Sánchez, J. Contreras García, A.J. Cohen, W. Yang, NCI : revealing non-covalent interactions, J. Am. Chem. Soc. 132 (2010) 6498–6506.

[46] J. Contreras-García, E.R. Johnson, S. Keinan, R. Chaudret, J.P. Piquemal, D.N. Beratan, W. Yang, NCIPLOT: A program for plotting noncovalent interaction regions, J. Chem. Theory Comput. 7 (2011) 625–632.

[47] R.G. Barradas, S. Fletcher, J.D. Porter, The hydrolysis of maleimide in alkaline solution, Can. J. Chem. 54 (1976) 1400–1404.

[48] Y. Imai, H. Itoh, K. Naka, Y. Chujo, Thermally Reversible IPN Organic - Inorganic Polymer Hybrids Utilizing the Diels - Alder Reaction, Macromolecules. 33 (2000) 4343–4346.

[49] Q. Tian, Y.C. Yuan, M.Z. Rong, M.Q. Zhang, A thermally remendable epoxy resin, J. Mater. Chem. 19 (2009) 1289–1296.

[50] V. Gaina, O. Ursache, C. Gaina, E. Buruiana, Novel Thermally-Reversible Epoxy-Urethane Networks, Des. Monomers Polym. 15 (2012) 63–73.

[51] S. Vyazovkin, N. Sbirrazzuoli, Mechanism and Kinetics of Epoxy−Amine Cure Studied by Differential Scanning Calorimetry, Macromolecules. 29 (1996) 1867–1873.

[52] V.D. Kiselev, E.A. Kashaeva, M.S. Shihab, L.N. Potapova, G.G. Iskhakova, Diffusion control of the Diels — Alder reaction rate at elevated pressures, Russ.Chem.Bull. 53 (2004) 45–50.

[53] O. Ursache, C. Gaina, V. Gaina, C.D. Varganici, Thermal properties of thermorensponsive networks based on polyurethanes, Rev. Roum. Chim. 61 (2016) 379–384.

[54] Q. Tian, M.Z. Rong, M.Q. Zhang, Y.C. Yuan, Optimization of thermal remendability of epoxy via blending, Polymer. 51 (2010) 1779–1785.